COBEM 2025
28TH INTERNATIONAL CONGRESS OF MECHANICAL ENGINEERING
ABCM Brazilian Society of Mechanical Sciences and Engineering
28th ABCM International Congress of Mechanical Engineering
November 09-11, 2025, Curitiba-PR, Brazil

COB-2025-0365
HEAT TRANSFER IN POROUS MEDIA WITH APPLICATION IN VOLUMETRIC RECEIVERS OF HELIOSTAT PLANTS

Carlos de jesus Silva de Oliveira
d2024007762@unifei.edu.br

Paulo Mohallem Guimarães
pauloguimaraes@unifei.edu.br

Rogério Fernandes Brito
rogbrito@unifei.edu.br

Ricardo Luiz Perez Teixeira
ricardo.luiz@unifei.edu.br

Carlos Henrique de Oliveira
carloshenrique.unifei@gmail.com

Federal University of Itajubá - Itabira Campus
Rua Irmã Ivone Drumond, 200, Distrito Industrial II, Itabira, Zip.: 35903-087, MG, Brazil

Abstract. *This study investigates the heat transfer within foams, focusing on their application in volumetric receivers for solar power plants that use concentrated solar radiation. Solar radiation from a heliostat field is concentrated onto receivers located at the top of a tower. The receiver system consists of multiple components: a secondary concentrator, a glass window, an absorber media, and an external pressurized vessel. The secondary concentrator directs solar radiation onto the glass window, which allows the radiation to pass through to the absorber porous media inside the pressurized receiver. This porous matrix transfers heat to the working fluid, which in this study is pressurized air. The cooler pressurized air enters the receiver's confined inlet and exits through the outlet at a higher temperature. The heated air is then utilized in thermodynamic cycles to generate electricity. A numerical simulation tool (COMSOL MULTIPHYSICS®) is used to model and approximate solutions to improve the receiver's thermal efficiency, taking into account radiation, convection, and conduction heat transfer in both laminar and turbulent flow regimes within the porous structure. The model incorporates parameters like porosity and thickness of the porous media. The mathematical model and numerical methods are validated against benchmark problems from existing literature. While porosity can enhance heat transfer by acting as an absorber, it can also cause a pressure drop that may affect the overall process. Various materials are examined as porous absorber media, including ceramic, alumina, and graphene. Additionally, factors such as radiation intensity, matrix thickness, and porosity are varied. The results show that the porous media significantly increases the contact area between the heated air and the solid conductive material, improving heat transfer. This study shows that inlet velocity is the most influential parameter affecting THETAMAX in a volumetric receiver. Increasing the velocity from 0.2 to 1.5 m/s drastically reduces THETAMAX, especially at lower velocities, due to enhanced convective cooling. Porosity and permeability play a smaller but supportive role—higher porosity (≈0.95) with good permeability slightly improves thermal performance, especially when velocity is already high. On the other hand, heat flux directly raises THETAMAX in a nonlinear fashion. Temperatures increase slowly at low flux but rise steeply above 75,000 W, indicating the importance of flux control to prevent overheating. The ideal operating range for thermal stability and realistic performance is: Inlet velocity ≥ 1.2 m/s, Porosity ≈ 0.95, Heat flux ≈ 75,000 W*

Keywords**:** Heliostat Plant, Volumetric Receiver, Porous Matrix, Convection heat transfer

1. INTRODUCTION

Clean and renewable energy has become a global priority due to the limitations of fossil fuels and the growing demand for power. Among renewable sources, solar energy stands out for its abundance, clean use, and accessibility. To address challenges like low energy density and conversion inefficiency, concentrated solar power (CSP) has emerged as a key technology for electricity generation.

The main source of CSP is the more abundant energy in the environment, the sun. There are four technology types: Parabolic, Dish, Central Tower and Fresnel. Central tower power plants with volumetric concentrator have shown high performance in the production of clean and cheap energy.

A study by Behar (2013) analyzed research related to solar thermal power plants with central receiver, indicating that systems with volumetric receiver technology have great energy potential. In turn, Avila-Martin (2011) reviewed types of volumetric receivers, indicating the receiver from REFOS program as the most efficient. Albanakis (2009) studied types of porous materials which have better performances in thermal energy convection to the system fluid.

The study of Buck (2001) demonstrated that plants using volumetric central receiver has the potential to compete in today's market. In 2031, one system with central volumetric receiver was built by Del Río. Currently, It is on the first test phase using part of the solar field of Solugas. Later, this innovation will be applied to the Abengoa plant, allowing its entry into the market and reducing the cost of energy.

According to the CSP Gen3 roadmap, raising operating temperatures above 700 °C is essential to reach 50% solar-to-electricity efficiency (Mehos et al., 2017; He et al., 2020). Solar receivers, directly irradiated by solar radiation, play a key role in boosting efficiency and lowering the Levelized Cost of Energy (Li and Tao, 2017; Dowling et al., 2017). Among receiver types, the volumetric receiver stands out by distributing solar flux into a 3D porous medium, allowing higher flux limits and efficient absorption through both the fluid and porous matrix.

Porous structures such as honeycombs, wire meshes, packed beds, and foams made of metallic or ceramic materials are widely used in volumetric receivers. Concentrated solar radiation penetrates and is absorbed within the porous medium, while the heat transfer fluid (usually air) exchanges heat with it, producing the so-called volumetric effect (Kribus et al., 2014, A and B). Despite their efficiency in solar-to-thermal conversion, challenges such as multiscale modeling, multiple heat transfer mechanisms, and dependence on geometry and material properties make experimental and numerical analyses complex, leading to ongoing studies on performance enhancement in CSP applications.

In the present work, it is performed a numerical heat transfer study using metallic foams with application in volumetric receivers applied in solar plants. The working fluid is pressurized air. A numerical simulation package (COMSOL MULTIPHYSICS ®) is used in order to approximate solutions as an attempt to improve thermal efficiency of the receiver by considering convection and conduction heat transfer in laminar and turbulent (k-ω) regimes inside a volumetric receiver through a porous structure that has a certain porosity and thickness. Heat flux is prescribed on the absorber surface as a mean of considering the solar irradiation source. The mathematical model and the numerical techniques are validated with a benchmark problem found in literature. Also, the laminar and turbulent models are considered to take into consideration the high pressurized air at the entrance of the volumetric receiver. It is known that porosity may enhance heat transfer by working as an absorber media. However, the porous media may induce a pressure drop that may interfere in the whole process that may bring structure damage. Some materials are studied as porous absorber media: Alumina, silicon carbide. It is observed that the porous media strongly plays its role to increase the contact area of air to be heated and the solid conductive material.

2. RECEIVER DESIGN AND PROBLEM FORMULATION

The problem consists of a volumetric receiver, considering steady laminar and turbulent forced convection. This first analysis takes into consideration air as the working fluid and Silicon Carbide and Alumina as the solid materials in the porous media matrix. Figure 1 depicts the geometry and the boundary conditions of the problem. The computational domain consists of four subdomains that are signalized by the squares in Fig. 1. These subdomains are the air domain (regions 1, 2 and 3) and the porous media domain (region 4). Table 1 shows the properties of Silicon Carbide, Alumina and air, respectively. The boundary conditions are shown by the circles which are related to the surfaces the circles are in contact with.

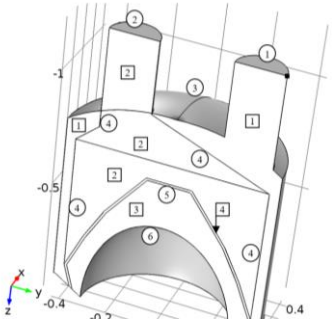

Figure 1. Geometry and boundary conditions.

Surface 1 : inlet: Pressurized air velocity (V_0): 0.5m/s (Silicon Carbide) and 0.01 (Alumina), temperature (T_0): 293.15 K; Surface 2: outlet: developed flow conditions; Surface 3, 4, 6: outer walls: no-slip condition, thermal isolation; Surface 5: Temperature: 800K (Silicon Carbide); Heat Flux: 10,000 to 150,000 W/m^2.

All surfaces belonging to the cut plane are under symmetry conditions (flow and heat symmetry).

Table 1. Properties of Silicon Carbide and Alumina.

	Silicon Carbide	Alumina	Un.
Heat capacity at constant pressure	900	900	J/(kg*K)
Density	3100	3900	kg/m^3
Thermal conductivity	150	27	W/(m*K)
Permeability	0.0001	0.5	m^2
Ratio of specific heats	1	1	1
Dynamic viscosity	1	1	Pa*s
Young's modulus	300e9	300e9	[Pa]
Poisson's ratio	0.14	0.222	-

On the surfaces interfacing two different domains, appropriate boundary conditions are imposed in relation to one another. The basic governing equations for mass momentum and energy conservations (without the turbulence treatment) for the fluid domain are, respectively:

$$\nabla.(\rho\mathbf{u})=0 \tag{1}$$

$$\rho(\boldsymbol{u}.\nabla)\boldsymbol{u}=\nabla.\left[-p\boldsymbol{I}+\mu(\nabla\boldsymbol{u})+(\nabla\boldsymbol{u})^T-\frac{2}{3}\mu(\nabla\boldsymbol{u})\boldsymbol{I}\right] \tag{2}$$

$$\rho C_p\boldsymbol{u}\nabla T=\nabla.(k\nabla T) \tag{3}$$

where $\boldsymbol{u}$ is the fluid velocity vector, ρ is the fluid density, $\boldsymbol{I}$ is the identity vector, μ is the dynamic viscosity, *Cp* is the specific heat, *k* is the fluid thermal conductivity, *p* is the pressure and *T* the is the temperature.

The governing equations for the porous matrix (Brinkman's equations) are:

$$\frac{\rho}{\varepsilon_p}\left((\boldsymbol{u}.\nabla)\frac{\boldsymbol{u}}{\varepsilon_p}\right)=\nabla.\left[-p\boldsymbol{I}+\frac{\mu}{\varepsilon_p}\left(\nabla\boldsymbol{u}+(\nabla\boldsymbol{u})^T\right)-\frac{2\mu}{3\varepsilon_p}(\nabla.\boldsymbol{u})\boldsymbol{I}\right]-\left(\mu K^{-1}+\beta_F|\boldsymbol{u}|+\frac{Q_{br}}{\varepsilon_p^2}\right)\boldsymbol{u} \text{ and } \rho\nabla.\boldsymbol{u}=Q_{br} \tag{4}$$

where ε_p is porosity and *K* is the permeability.

Finally, the heat transfer equations in porous media are given by:

$$\rho C_p\boldsymbol{u}\nabla T=\nabla.(k_{eq}\nabla T) \text{ and } k_{eq}=\theta_p k_p+(1-\theta_p)k \tag{5}$$

where θ_p is the volume fraction, k_p is the effective thermal conductivity fluid of the fluid-solid mixture.

3. VALIDATION

One of the validations was the porous media problem whose results were contrasted with the ones by Hossain and Wilson (2002). It is a study of natural convection in a square cavity containing porous medium. T_c is the temperature on the cold surfaces and T_h is the temperature on the heated surfaces. There is a region on the bottom right vertical wall where the temperature varies linearly. This validation can be found in Comsol Multiphysics ® documentation. Temperature and velocities behaviors are contrasted. There is an excellent agreement.

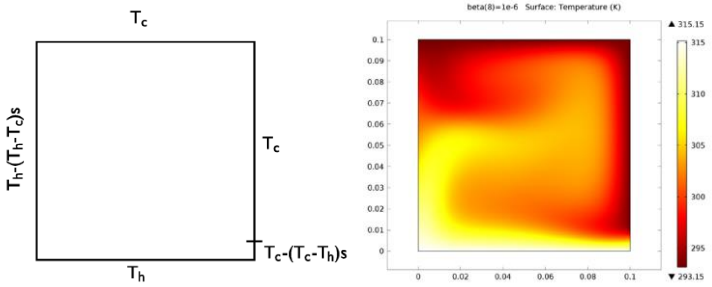

Figure 2. Geometry, boundary conditions and the isotherms for Rayleigh number equal to 10^5.

4. NUMERICAL METHOD

The Comsol Multiphysics was used to approximate solutions to the governing equations. The finite element method is used. Figure 3 shows the meshes and Table 2 shows the mesh statistics for the two cases.

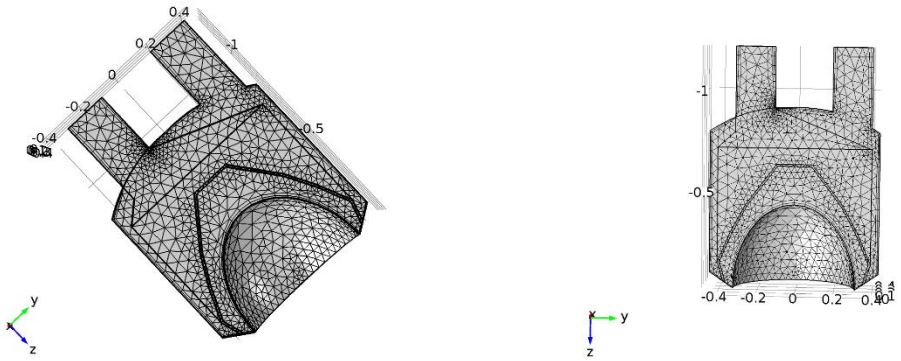

a) Laminar regime b) Turbulent regime

Figure 3. Mesh with tetrahedrical elements.

Table 2. Mesh statistics.

Property	Value
Laminar Regime – Silicon Carbide	
Minimum element quality	0.007453
Average element quality	0.5319
Tetrahedral elements	46403
Pyramid elements	1012
Prism elements	10496
Triangular elements	9810
Quadrilateral elements	428
Edge elements	975
Vertex elements	61

Property	Value
Turbulent Regime - Alumina	
Minimum element quality	0.005496
Average element quality	0.5349
Tetrahedral elements	46360
Pyramid elements	1012
Prism elements	10496
Triangular elements	9788
Quadrilateral elements	428
Edge elements	975
Vertex elements	61

5. RESULTS

5.1 Results for laminar regime

Figure 4 shows the thermal field of the four domains: a) entrance zone where air enters the system and goes until it reaches the porous media, b) exit zone which is the domain after leaving the porous media , c) intermediate zone which is the domain between the glass dome and the porous media and d) the porous matrix. The entrance region (a) temperature varies from 293 to 800k. This more heated region is placed on the lower region that is in contact with the porous region surface that is at 800 K. Air is significantly heated as it passes through the porous region. In the exit region (b), that is the region after the porous matrix, temperature ranges from 621K to 796K. It is worth seeing that the coldest place in this region is in its lower part. There was about a 273% temperature increase when comparing to the inlet air temperature of 293.15K. This is due to the porous medium effect that plays a role of augmenting the thermal contact between air and the porous material. Region (c) presents almost a uniform temperature of 800K. The thickness of this porous layer is small and the solid material used with moderate thermal conductivity (k = 27 W/m.K). An interesting study here is to optimize the thickness of this porous matrix in order to achieve the best heat transfer possible taking into consideration pressure load gained and material cost.

Figure 5 shows the streamlines for the case from Fig. 4. For a velocoity entrance of 0.5 m/s, the flow field seems to be organized with no significative recirculations. One can observe the air passing thorugh the porous media. This geometry assures that the air (red lines) moves from the entrance tube and then flows over the internal chamber and then reaches the lower porous media inlet. It seems to be interesting to analyse the velocity field to check if air flow is uniform on the porous media inlet.

Figure 6 presents the velocity field for the four domains for the case from figure 4. For the porosity of 0.4, the exit velocity is almost four times bigger than the entrance velocity, although the tubes have the same diameter. It is interesting to analyse in future works the air compressibility for this kind of systems. In this test case, air is considered incompressible. As expected, the velocities in the porous media are lower. Due to the incompressibility effect, higher velocity regions have lower pressure fields (see Figure 7). One point that must be taken into consideration for future

studies is the high pressure difference in the porous matrix. Silicone Carbide is being used in the porous matrix as due to it supports great pressure differences, thermal shock and water hammers caused by turning on and off of turbines in the net.

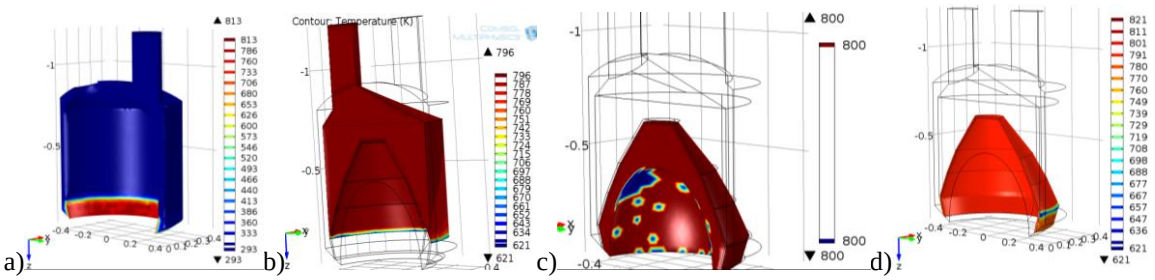

Figure 4. Isotherms for the four domains (V_0 = 0.5 m/s, T_0 = 293.15K, T_{matrix} = 800K and p_0 = 15 bar)

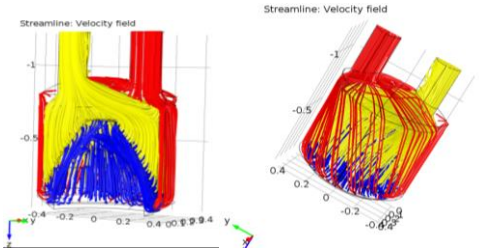

Figure 5. Streamlines (V_0 = 0.5 m/s, T_0 = 293.15K, T_{matrix} = 800K and, p_0 = 15 bar)

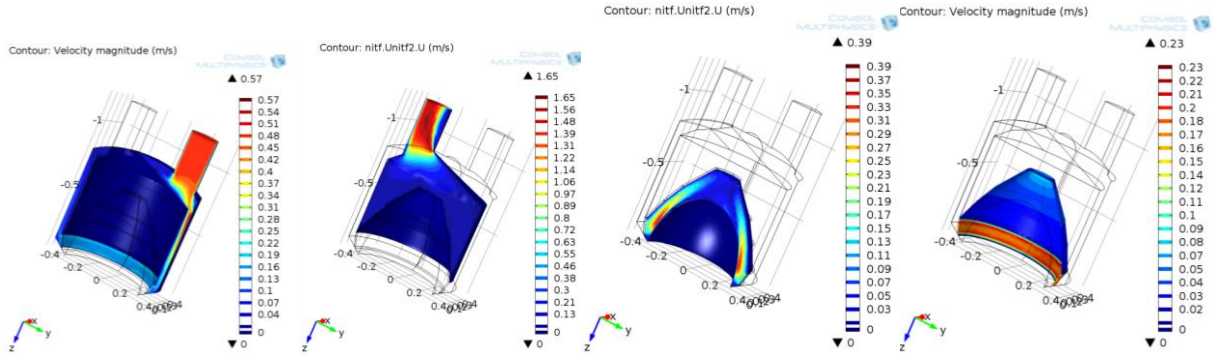

Figure 6. Velocity field (V_0 = 0.5 m/s, T_0 = 293.15K, T_{matrix} = 800K and p_0 = 15 bar)

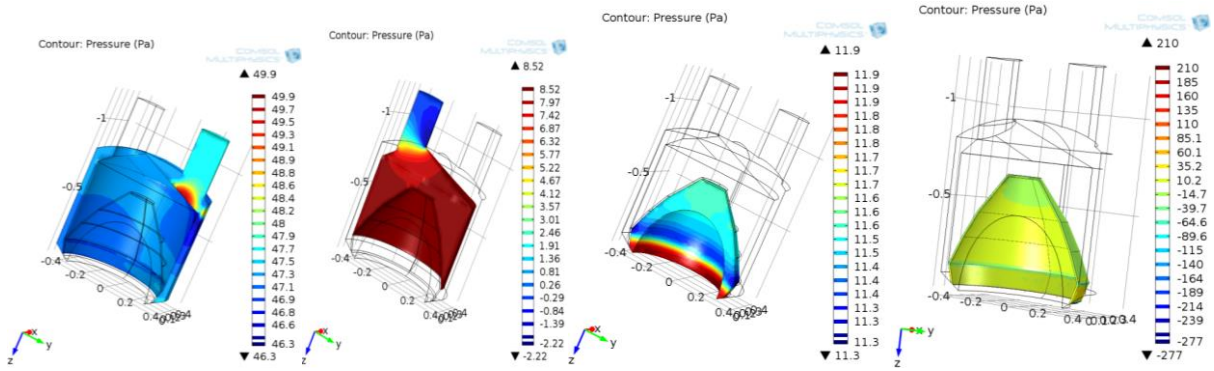

Figure 7. Pressure field (V_0 = 0.5 m/s, T_0 = 293.15K, T_{matrix} = 800K and p_0 = 15 bar)

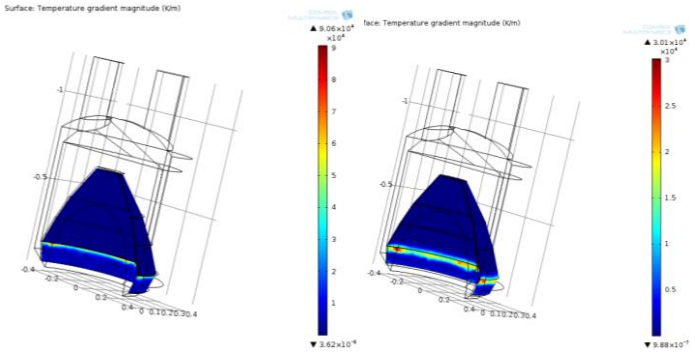

a) Inner surface of the porous media b) Outer surface of the porous media

Figure 8. Temperature gradients of the inner and outer surfaces of the porous media (V_0 = 0.5 m/s, T_0 = 293.15K, T_{matrix} = 800K and p_0 = 15 bar)

In Fig. 8, one can see the behavior of the temperature gradients of the porous material on its inner and outer surfaces. Just in accordance with the temperature field, there are greater gradients near the upper part of the lower entrance region. Figure 9 also depicts the gradient temperatures inside the porous media.

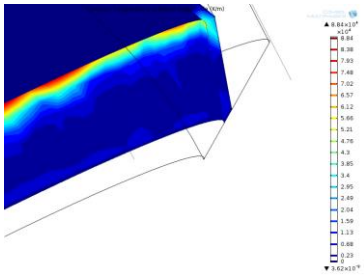

Figure 9. Temperature gradients of the porous media (V_0 = 0.5 m/s, T_0 = 293.15K, T_{matrix} = 800K and p_0 = 15 bar)

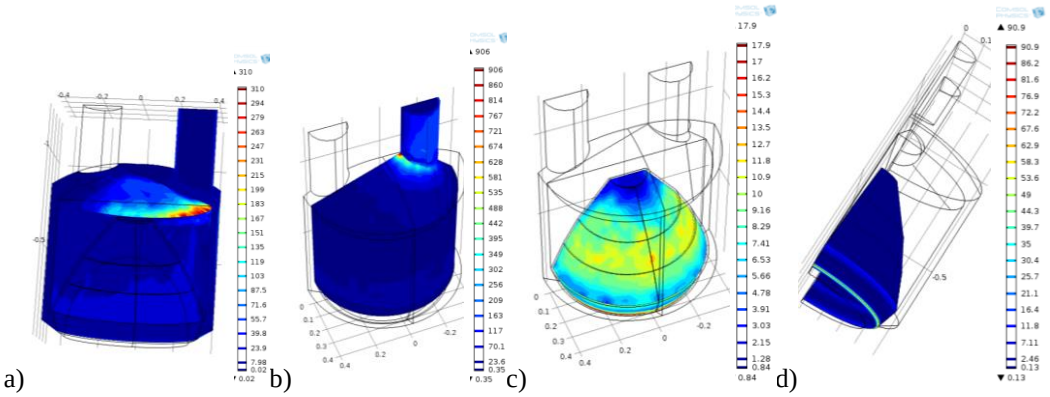

a) b) c) d)

Figure 10. Shear rate behavior.

Figure 10 shows the shear rate in the entrance domain (a), the exit domain (b), the intermediate domain (c) and the porous matrix domain. Shear rate is the rate at which a progressive shearing deformation is applied to some material or to the walls. As expected, borders are likely to have higher shear stresses. One may note that in the shear stress is not related to the field with highest pressure. For instance, the domain with highest average shear stress is the exit domain whereas the region that presents the highest average pressure field is the porous media. However, the field that shows the highest is the one with higher average temperatures.

Finally, Figure 11 depicts the conductive and convective heat fluxes in the porous media. Heat convection is clearly higher in the bottom of the matrix. When the fluid passes through the bottom, this region is already heated and then the fluid passes through the porous matrix again, to find its path to the exit region.

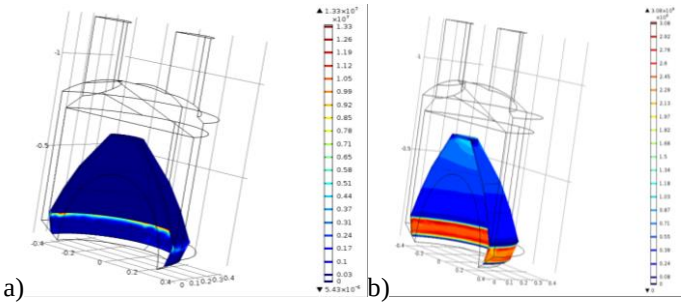

a) b)

Figure 11. Conductive (a) and convective (b) heat fluxes in the porous media.

5.2 Results for turbulent regime

Figures 12 to 15 consider turbulence models for Alumina and permeability of 0.5m^2. Also, the entrance uniform velocity is 0.01m/s. One can see in Figure 12 that for the boundary conditions used, the streamlines do not show a flow featuring a turbulent regime with vortices. This is due, for a first analysis, the entrance velocity (0.01m/s) and heat flux (100W/m^2) which may induce laminar features. When implementing a turbulent model, many attempts were carried out to reach solution. That is why smooth boundary conditions were here. In a future work, a sweep analysis is going to be used to reach higher entrance velocities and more real heat fluxes.

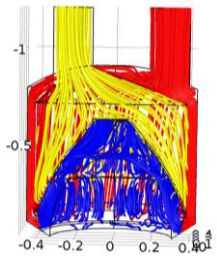

Figure 12. Streamlines for the three domains.

Figure 12 depicts the temperature field. The maximum temperature is 361 K in this domain and it happens in the exit to the porous media where heat flux is applied. It is important to mention that the inner walls are considered adiabatic and is why the cold air entering the system is not heated. This situation is different from what happens in the real problem. A more appropriate boundary condition must be applied at such walls such as similar temperature as the inner heated air near the inner wall. This is material for future approach. The maximum temperature is quite below the maximum temperature found for the laminar case due to the materials are different and also in the laminar case, it was specified temperature of 800K in the absorber surface. In addition to this, the entrance velocity is 0.01m/s compared to 0.5m/s for the laminar case.

Figure 13 (a) shows the temperature field for the porous matrix. A maximum value of 532K is achieved which is much lower than for the laminar case due to the reasons already mentioned before. It is interesting to observe how the temperature rises as one move to the center of the matrix. This is in consonance with the temperature in Fig. 13 (b). When comparing the behavior in Fig. 13 (b) (heat flux imposed in the absorber surface) with Fig. 4 (temperature imposed in the absorber surface), in the same porous domain, the case with uniform temperature on the absorber surface shows quite a uniform temperature in the whole matrix. While for the heat flux boundary condition, the temperature field gradually rises from 350K to 532K. It seems there is a higher temperature gradient when heat fluxes are imposed. The temperature values for the temperature imposed are higher, though.

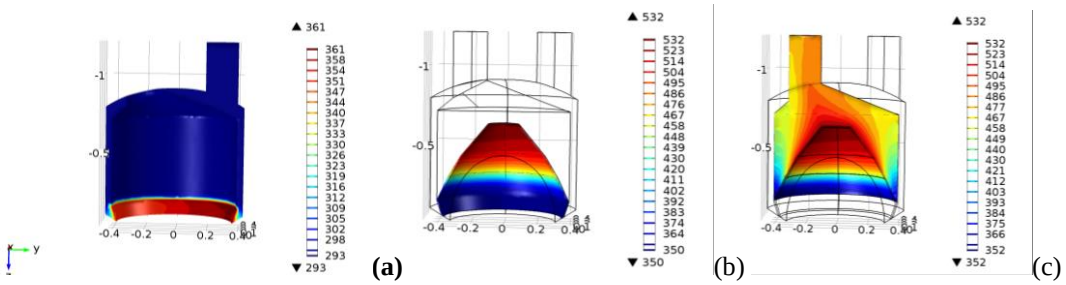

(a) (b) (c)

Figure 13. Temperature field for: a) the entrance domain, b) in the porous matrix, c) after porous matrix

Figure 13 (c) shows the temperature field of air exiting the porous media and flow through the exit domain. Some similar features are found here as in Figure 13 (b) when it comes to the temperature gradient. Also, the temperature becomes higher when approaching the core of this domain. It seems that the thermal behavior for heat flux as boundary condition is in more agreement with what happens in real situation when comparing to the temperature-imposed boundary conditions.

Some comparisons are interesting, however that it is important to mention the differences taken into consideration such as the material and order level of temperature and heat flux imposed. As a general comprehension, the different behaviors are in accordance with literature, though.

5.3 Analysis of the Effect of the Inlet Velocity for turbulent regime

In this section, a parametric study is carried out to check the effect of velocity in the temperature field. Table 3 shows some parameters in the current section. We now will name cases. The material used here is Graphene. The THETAMAX is taken from domain after the porous matrix, that is, domain 2. Some values may appear too high or too small compared to real situations. Since it is a parametric study such approach is totally comprehensive.

Table 3. THETAMAX versus Varied Inlet Velocity

Case	Porosity	Permeability (m^2)	Inlet Velocity (m/s)	Heat Flux (W/m^2)	THETAMAX (K)
1	0.95	0.00000001	0.2	75000	11000
2	0.95	0.00000001	0.5	75000	4061
3	0.95	0.00000001	0.8	75000	2804
4	0.95	0.00000001	1.2	75000	2074
5	0.95	0.00000001	1.5	75000	1772

The data reveal a strong inverse relationship between inlet velocity and THETAMAX in the volumetric receiver. With porosity and permeability held constant (0.95 and $1\times10^{-8}\,m^2$, respectively), increasing the inlet velocity from 0.2m/s to 1.5 m/s under a constant heat flux of 75,000 W/m^2 results in a sharp decrease in maximum temperature—from 11,000 K to 1,772 K. The most significant drop occurs at low velocities, indicating a highly non-linear thermal response in this range. Beyond 1.0 m/s, further increases in velocity yield smaller reductions in THETAMAX, showing diminishing returns. Among the cases presented, the data for inlet velocities of 1.2 m/s and 1.5 m/s, with THETAMAX values between 2,074 K and 1,772 K, are the most representative of real operating conditions, where thermal control is critical to maintaining structural integrity and system efficiency. This emphasizes the importance of working with moderate to high velocities to optimize thermal performance without compromising practical flow requirements.

5.4 Analysis of the Effect of Porosity for turbulent regime

In this section, a parametric study is carried out to check the effect of porosity in the temperature field. Table 4 shows some parameters in the current section. We now will name cases. The material used here is Graphene. The THETAMAX is taken from domain after the porous matrix, that is, domain 2. Some values may appear too high or too small compared to real situations. Since it is a parametric study such approach is totally comprehensive.

Table 4. THETAMAX versus Varied Porosity

Case	Porosity	Permeability (m^2)	Inlet Velocity (m/s)	Heat Flux (W/m^2)	THETAMAX (K)
6	0.6	0.0000000001	1.5	75000	1781
7	0.7	0.0000000005	1.5	75000	1819
8	0.8	0.000000009	1.5	75000	1779
9	0.9	0.000000005	1.5	75000	1781
10	0.95	0.00000008	1.5	75000	1775

In this set of cases, THETAMAX remains relatively stable despite variations in porosity from 0.60 to 0.95 and accompanying changes in permeability. All cases were run at a fixed inlet velocity of 1.5 m/s and heat flux of 75,000 W/m^2. THETAMAX fluctuates only slightly, ranging from 1,775 K to 1,819 K, suggesting that under high inlet velocity, the effect of porosity and permeability on maximum temperature becomes less dominant. Notably, case 7 (porosity 0.70, permeability $5\times10-10^5$) shows a slightly higher THETAMAX (1,819 K), likely due to limited fluid flow and reduced convective heat transfer at that specific combination. The most realistic scenario appears to be case 10 (porosity 0.95, permeability 8×10^{-8}), with THETAMAX at 1,775 K. This aligns with previous findings and supports the conclusion that high porosity combined with reasonable permeability and inlet velocity enables effective thermal control in volumetric receivers.

5.5 Analysis of the Effect of Heat Flux for turbulent regime

In this section, a parametric study is carried out to check the effect of heat flux in the temperature field. Table 5 shows some parameters in the current section. We now will name cases. The material used here is Graphene. The THETAMAX is taken from domain after the porous matrix, that is, domain 2. Some values may appear too high or too small compared to real situations. Since it is a parametric study such approach is totally comprehensive.

Table 5. THETAMAX versus Varied Heat Flux

Case	Porosity	Permeability (m^2)	Inlet Velocity (m/s)	Heat Flux (W/m^2)	THETAMAX (K)
11	0.95	0.0000000001	2	10000	447
12	0.95	0.0000000001	2	25000	680
13	0.95	0.0000000001	2	30000	912
14	0.95	0.0000000001	2	75000	1455
15	0.95	0.0000000001	2	100000	1834
16	0.95	0.0000000001	2	150000	2615

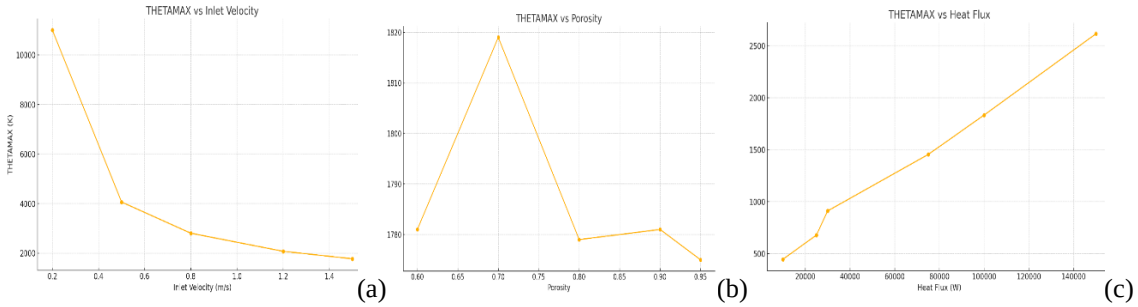

(a) (b) (c)

Figure 14. THETAMAX versus Varied Inlet Velocity (a), Porosity (b), and Heat Flux (c).

The results reveal a clear and strong positive correlation between heat flux and THETAMAX in the volumetric receiver. With constant porosity (0.95), permeability ($1\times10^{-10}m^2$), and inlet velocity (2.0 m/s), increasing the heat flux from 10,000 to 150,000 W/m^2 leads to a steep rise in maximum temperature—from 447 K to 2,615 K. The temperature increase is nonlinear, becoming steeper as the heat flux exceeds 75,000 W/m^2, indicating the system's growing thermal sensitivity to radiative input at higher loads. This suggests that while moderate heat flux levels (such as 75,000–100,000 W/m^2) can offer effective energy capture with controlled temperatures, extreme values like 150,000 W/m^2 may risk overheating and require enhanced cooling or material limits. Among the cases, 75,000 W/m^2 (THETAMAX = 1,455 K) appears most representative of real-world operating conditions, where a balance is needed between thermal efficiency and material safety. This highlights the critical importance of tuning heat input to the receiver's cooling capacity.

6. CONCLUSION

This work studies the mixed convection heat transfer in a laminar and turbulent regimes inside a volumetric receiver used in concentrating solar power plants using Silicon Carbide in the laminar case and Alumina in the turbulent case. Although this is a subject already developed in some countries such as Spain, Germany, USA, Brazil does not have its plant yet. That is why it is so important to stimulate students and teachers on this field. It is a promising clean energy source that can be successfully implemented in Rankine and Brayton cycles, for instance. Therefore, the main contribution of this work is to learn the physics and a mathematical model that are used in this problem and the basic temperature, velocity, and pressure behaviors of the work fluid. Air is significantly heated as it passes through the porous region. In the exit region, that is the region after the porous matrix, temperature ranges from 621K to 796K for the laminar case with temperature-imposed boundary condition. It is worth seeing that the coldest place in this region is in its lower part. There was about a 273% temperature increase when comparing to the inlet air temperature of 293.15K. For the turbulence case, where heat flux is imposed, the temperature behavior in the porous matrix as well as in the exit domain shows a gradient temperature different from that in the laminar case when temperature is imposed as boundary condition. The case with flux imposed to take into consideration as a means of considering the radiation on the absorber surface in the porous matrix seems to be in more accordance with what happens in a real situation and with literature. In a turbulent case, for Alumina, with the entrance velocity (0.01m/s) and heat flux ($100W/m^2$), the temperature becomes higher when approaching the core of porous domain. It seems that the thermal behavior for heat flux as boundary condition is in more agreement with what happens in real situation when comparing to the temperature-imposed boundary conditions.

Finally, this study analyzed the influence of **inlet velocity**, **porosity/permeability**, and **heat flux** on the maximum temperature (THETAMAX) within a volumetric solar receiver, under different controlled scenarios, as follows:
1. Effect of Inlet Velocity (Porosity = 0.95, Permeability = $1\times10-8$ m^2): As inlet velocity increased from 0.2 m/s to 1.5 m/s, THETAMAX dropped dramatically from 11,000 K to 1,772 K. The cooling effect was strongest at low velocities, with diminishing temperature reduction at higher velocities. Realistic operational values were observed at 1.2–1.5 m/s, where THETAMAX remained below 2,100 K—more manageable for receiver materials; **2. Effect of Porosity and Permeability** (Inlet Velocity = 1.5 m/s): With increasing porosity (0.6 to 0.95) and varying permeability, THETAMAX remained relatively stable, ranging from 1,775 K to 1,819 K. This suggests that in high-velocity regimes, the influence of porosity and permeability on peak temperature becomes less dominant. Among all, porosity of 0.95 with higher permeability provided the lowest THETAMAX (1,775 K), reinforcing its suitability in real applications; **3. Effect of Heat Flux** (Inlet Velocity = 2 m/s, Porosity = 0.95): As heat flux increased from 10,000 to 150,000 W/m^2, THETAMAX rose sharply from 447 K to 2,615 K. The relationship was nonlinear, with faster temperature escalation at high flux levels. A heat flux of 75,000 W/m^2 yielded THETAMAX ≈ 1,455 K, which appears to be a realistic and safe operating point, balancing energy input with thermal limits. Combining the three effects, the most thermally stable and realistic operating point for a volumetric receiver is achieved with: High inlet velocity (≥1.2 m/s), High porosity (~0.95) with sufficient permeability, Moderate heat flux (≈75,000 W/m^2). This configuration yields THETAMAX values in the range of 1,400–1,800 K, which are thermally efficient and structurally sustainable. Such a setup supports optimal absorber performance while minimizing the risk of thermal damage, enabling long-term operation and reliability of solar thermal systems.

7. ACKNOWLEDGEMNTS

The authors thank **FAPEMIG** (Process: APQ-02457-12) and **LEFTER100** (Laboratory of Computational, Experimental and Numerical Thermal and Fluid Engineering) at UNIFEI, Itabira Campus, Minas Gerais, Brazil.

8. REFERENCES

Albanakis, C., Missirlis, D., Michailidis, N., Yakinthos, K., Goulas, A., Omar, H., Tsipas, D., Granier, B., 2009. "Experimental analysis of the pressure drop and heat transfer through metal foams used as volumetric receivers under concentrated solar radiation". Experimental Thermal and Fluid Science, Vol. 33, pp. 246–252.

Ávila-Marín, A. L., 2011. "Volumetric receivers in Solar Thermal Power Plants with Central Receiver System technology: A review". Solar Energy, Vol. 85, pp. 891–910.

Behar, O.; Khellaf, A.; Mohammedi, K., 2013. "A Review of studies on central receiver solar thermal power Plants". Renewable and Sustainable Energy Reviews, Vol. 23, pp. 12–39.

Buck, R., Bra¨uning, T., Denk, T., Pfa¨nder, M., Schwarzbo¨zl, P., Tellez, F., 2002. Solar-Hybrid Gas Turbine-based Power Tower Systems (REFOS). In Proceedings of the ASME 201 at Forum 2001, Solar Energy: The Power to Choose, April 21–25, 2001, Washington, DC.

Del Río, A., Korzynietzb, R., Briosoa, JA., Gallasa, M.,. Ordóñeza, I., Queroa, M., and Díaza, C. "Soltrec - Pressurized volumetric solar air receiver technology"

Dowling, A.W., Zheng, T., Zavala, V.M., Economic assessment of concentrated solar power technologies: a review, Renewable Sustainable Energy Rev. 72 (2017) 1019–1032, https://doi.org/10.1016/j.rser.2017.01.006.

He, Y.-L., Qiu, Y., Wang, K., Perspective of concentrating solar power, Energy 198 (2020), 117373, https://doi.org/10.1016/j.energy.2020.117373.

Hossain, M., Wilson, M., 2002. "Natural covectionn flow in a fluid-saturated porous medium enclosed by non-isothermal walls with heat generation". Internnational Journal of Thermal Sciences, Vol. 41, pp. 447-454.

Kribus, A., Grijnevich, M., Gray, Y., Parametric study of volumetric absorber performance, Energy Proc. 49 (2014) 408–417, https://doi.org/10.1016/j.egypro.2014.03.044.

Kribus, A., Gray, Y., Grijnevich, M., The promise and challenge of solar volumetric absorbers, Sol. Energy 110 (2014) 463–481, https://doi.org/10.1016/j.solener.2014.09.035. B

Li, M.-J., Tao, W.-Q., Review of methodologies and polices for evaluation of energy efficiency in high energy-consuming industry, Appl. Energy 187 (2017) 203–215, https://doi.org/10.1016/j.apenergy.2016.11.039.

Mehos M., Turchi C., Vidal J., Concentrating Solar Power Gen3 Demonstration Roadmap, National Renewable Energy Lab, 2017.

9. RESPONSIBILITY NOTICE

The authors are the only responsible for the printed material included in this paper.